Generation of regular waves with FPGA based controller in a wave channel

Batın DEMİRCAN^{1,3*}, Sabri BIÇAKÇI^{2,3}

¹Balikesir University, Institute of Science, Department of Electrical and Electronics Engineering, Cagis Campus, Balikesir, Turkey.

Geliş Tarihi (Received Date): 14.01.2025 Kabul Tarihi (Accepted Date): 25.03.2025

Abstract

Wave channel systems provide crucial experimental platforms for the development and optimization of wave energy converters. By enabling the safe and repeatable simulation of real ocean conditions, these systems play a key role in understanding wave behavior and reducing design risks. They allow the generation of a specific wave model to investigate the effects of water waves on coastal structures, coastal ecosystems, and offshore platforms. In this study, a hydraulically controlled piston-type wave generator was utilized in a 24-meter-long wave channel, which measures 1 meter in width and 1 meter in height, to produce regular waves. The wave generation system in the channel is operated by a hydraulic cylinder with a 400 mm stroke, controlled by a proportional directional control valve. An NI-CRIO 9074 programmable automation controller (PAC), featuring Field Programmable Gate Array (FPGA) technology and an NI-9263 analog output module with 15-bit resolution, was used for controlling the proportional directional control valve. The cylinder position was measured at 15-bit resolution using an NI-9215 analog input module. A proportional-integral control (PI) technique was implemented on the NI-CRIO 9074 hardware. The controller gains were determined experimentally, with a computer employed to perform real-time measurement and data logging of the generated waves. The entire system is managed by the NI-CRIO 9074 and regular wave production is achieved through LabVIEW-based user interface programs running on the computer.

Keywords: Wave channel, wave maker, FPGA, hydraulic system.

²Balıkesir University Faculty of Engineering, Department of Electrical and Electronics Engineering, Cagis Campus, Balıkesir, Turkey.

³Balıkesir University, Renewable Energy Research, Application and Development Center, Balıkesir, Turkey

^{*}Batın DEMİRCAN, batındemircan@gmail.com, http://orcid.org/0000-0002-0765-458X Sabri BIÇAKÇI, sbicakci@balikesir.edu.tr, https://orcid.org/0000-0002-2334-8515

Bir dalga kanalında FPGA tabanlı kontrolör ile düzenli dalgaların üretimi

Öz

Dalga kanalı sistemleri, dalga enerjisi dönüştürücülerinin geliştirilmesi ve optimizasyonu için kritik deneysel platformlar sunar. Gerçek okyanus koşullarının güvenli ve tekrarlanabilir şekilde simüle edilmesini sağlayan bu sistemler, dalga davranışının anlaşılmasında ve tasarım risklerinin azaltılmasında önemli rol oynamaktadır. Dalga kanalı sistemleri belirli bir dalga modelinin üretilmesini sağlayarak su dalgalarının kıyı yapıları, kıyı ekosistemleri ve açık deniz platformları üzerindeki etkilerinin anlaşılması için çalışmalarda kullanılmaktadır. Bu çalışmada toplam uzunluğu 24 metre, genişlik ve yüksekliği ise 1'er metre olan dalga kanalında düzenli dalgaların üretimi için hidrolik kontrollü ve piston tip dalga üretici kullanılmıştır. Dalga kanalında bulunan dalga üretici sisteminde 400mm stroka sahip hidrolik bir silindir ile oransal yön kontrol valfi tarafından kontrol edilmektedir. Dalga üretimi için oransal yön kontrol valfinin kontrolü için NI-CRIO 9074 paket kontrolcüsü (PAC), Field Programmable Gate Array (FPGA) donanımı yapısında ve NI-9263 analog çıkış modülü 15bit çözünürlükte kullanılmıştır. Silindirin konum bilgisi NI-9215 analog giriş modülü ile 15bit çözünürlükte ölçülmüştür. NI-CRIO 9074 donanımında kontrolör olarak oransal integral kontrol (PI) tekniği uygulanmıştır. Kontrolör katsayıların bulunmasında deneysel yöntem kullanılarak, üretilen dalgaların gerçek zamanlı olarak ölçüm ve kayıt edilmesinde bir bilgisayar kullanılmıştır. Tüm sistem NI-CRIO 9074 tarafından kontrol edilmektedir ve bilgisayarda LabVIEW tabanlı olarak geliştirilen kullanıcı ara yüz programları ile dalga kanalında düzenli dalga üretimi gerçekleştirilmiştir.

Anahtar kelimeler: Dalga kanalı, dalga üretici, FPGA, hidrolik sistem

1. Introduction

Wave energy has been attracting increasing attention among renewable energy sources due to its considerable potential and reliability. In contrast to solar and wind energy, which can experience intermittency, wave energy in certain regions can be utilized approximately 90% of the time [1]. This consistency stems from the continuous nature of ocean waves, which are perpetually driven by wind patterns and ocean currents, thereby rendering wave energy a more stable resource. Moreover, wave energy offers a high energy density per unit area, delivering notable advantages over other renewable sources [2]. Given the rising global energy demand and the urgent need for cleaner alternatives, wave energy stands out as a sustainable option to replace fossil fuels [3]. On the other hand, naturally occurring wind waves at sea can be captured to generate electricity through wave energy converters [4-7]. When examining wave channel systems, both circular and rectangular designs are commonly observed [8,9]. These channels typically employ "flap," "piston," or "plunger" type wave makers to produce waves [10].

Wave channels and analogous simulation setups play a critical role in advancing and optimizing wave energy converters, as they allow researchers to replicate oceanic wave conditions in a controlled setting and test the performance of various converter designs. Computational Fluid Dynamics (CFD) models, often termed numerical wave tanks, have

become indispensable tools in understanding wave behavior and its interaction with wave energy converters [11]. Studies have demonstrated that numerical simulations can closely mimic wave models and validate experimental data, thereby enhancing the design process for wave energy converter systems [12]. Furthermore, wave channels offer a platform to experimentally verify theoretical models under real-world conditions, ensuring that the resulting designs are robust and efficient. This iterative simulation-and-testing process is of paramount importance for advancing wave energy technologies and securing both reliability and efficiency in power generation [13].

Several studies in the literature reflect these developments. For instance, Khalid performed experimental research in a 12 m \times 0.6 m \times 0.6 m wave channel using the Omey Labs Wavemaker software and reported a servo motor-driven, piston-type wave maker controlled by NI-CRIO hardware. Parameters such as wave period and wave height were input into LabVIEW, and pressure measurements were taken at different depths (channel bottom, water surface, and above the free surface). The recorded pressure data were noted to closely approximate hydrostatic pressure, with increasing wave height corresponding to higher pressure values that approached the hydrostatic level [14]. In another study, Beneduce, examined a 30 m × 2.2 m × 0.88 m wave channel featuring two electric cylinders and a flap-type wave maker. The wave period was set between 0.5 s and 2.5 s, the water depth was kept at 0.7 m, and the maximum stroke of the hydraulic actuator was 0.5 m. The wave height obtainable with this stroke was estimated using first-order wave theory, and the tank's maximum wave-generation capacity was analyzed. In addition, flap analysis, calculations for the electric motor-driven hydraulic cylinder, and selection of mechanical components for the wave channel were carried out [15].

In another study conducted by Su et al., it was reported that a servo motor-driven pistontype wave maker was controlled using Rockwell Automation hardware components, and the control software was developed in C++ within a Windows environment. Additionally, irregular waves were generated using the JONSWAP spectrum via a wave measurement sensor placed 10 meters away from the wave maker [16].

In the context of precision position control of hydraulic cylinders, Jian-Jun et al. proposed a high-accuracy position control application for a double-acting, double-rod hydraulic cylinder. To enhance tracking performance and bandwidth, they developed a feedforward compensation based on the invariance principle using pole-zero placement theory. After modeling the system as a 4th-order discrete-time system, closed-loop Bode diagrams were examined with and without the feedforward structure. A sampling time of 2 ms was employed for the hydraulic cylinder, which had a total stroke of 1350 mm [17].

Ling et al. investigated PID control for a hydraulic system containing a single-rod, double-acting hydraulic cylinder and a servo valve. In their study, data were obtained using a 100-second excitation signal composed of three sinusoidal components, and an ARX [3-3-1] model was identified with 95% accuracy. Based on this model, the " K_p ," " K_i ," and " K_d " coefficients of the PID controller were determined using the Ziegler-Nichols method and tested in a simulation environment before being applied to the actual system [18].

Finally, Mahdi developed both a numerical model and a second-order transfer function with no zeros for a hydraulic cylinder in the Matlab/Simulink environment. The PID

controller parameters were tuned using Matlab's PID Tuner, yielding better results compared to manual tuning methods [19].

In this study, regular waves were generated using the wave channel located in the Hydraulic Laboratory of Balıkesir University's Civil Engineering Department. The wave generation system features a piston-type wave maker driven by a hydraulic servo cylinder. The position control of the hydraulic cylinder was achieved using the NI-CRIO 9074 PAC along with analog input and output modules. The control system utilized the FPGA embedded in the NI-CRIO 9074, employing a Proportional Integral (PI) control strategy. Real-time measurement of the generated waves was performed using wave probe sensors. In the scope of this study, Material and Methods are presented in Section 2, results are detailed in Section 3, and finally, the conclusions are discussed.

2. Materials and methods

2.1. Wave channel system

The wave generation system in the channel is of a piston-type structure. The wave maker is driven by a double-acting, double-rod hydraulic cylinder, with a total stroke length of 400 mm. The hydraulic system pressure is set at a constant 50 bar, maintained continuously using hydraulic accumulators to ensure system stability. The structure of the wave channel is illustrated in Figure 1. At the beginning of the wave channel, passive dampers are employed to suppress irregular waves at the rear of the wave maker during wave generation. At the end of the channel, both passive and coastal-type wave absorbers are used to mitigate the reflection of waves produced within the channel.

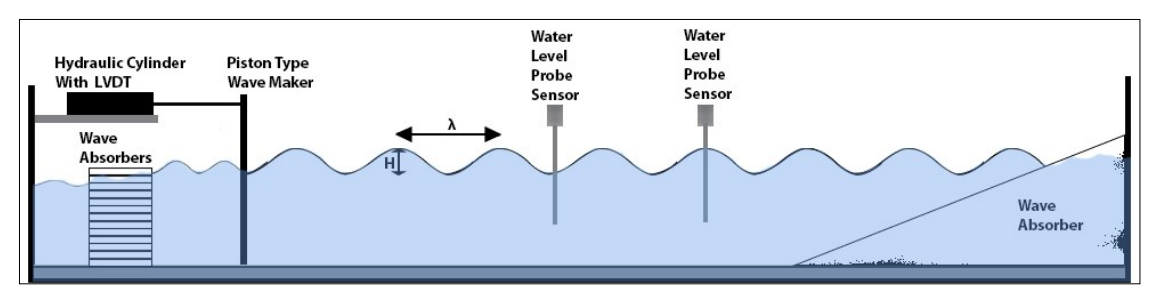


Figure 1. The structure of the wave channel

The mechanical, hydraulic, and electronic components of the wave channel in the laboratory environment are shown in Figure 2. For wave generation within the channel, the static water levels were set at 50 cm and 60 cm. Waves were generated with varying amplitudes and frequencies for different water levels.



Figure 2. The structure of the wave channel

The wave generation system used in the wave channel is referred to in the literature as a "piston-type" wave maker, which operates along a single axis. The movement range of the piston-type wave maker corresponds to that of the hydraulic cylinder, spanning 0–700 mm. In this study, the initial position of the wave maker was set at 500 mm, and wave generation was performed within the range of 300–700 mm. The physical structure of the piston-type wave maker driven by the hydraulic cylinder in the wave channel is shown in Figure 3.

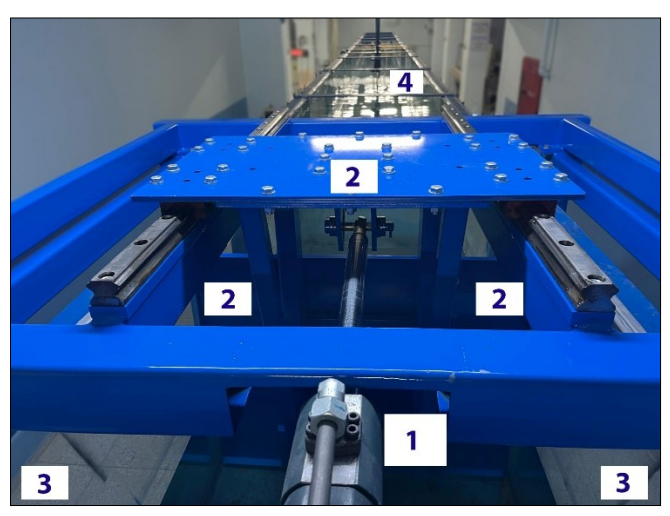


Figure 3. Top view of the wave maker: 1-hydraulic cylinder, 2-piston-type wave maker, 3-tank wall, 4-water surface

The waves generated in the wave channel propagate in a specific direction within the channel. Upon reaching the end of the channel, these waves collide with the channel wall, creating reflected waves after a certain period. To minimize the reflected waves at the end of the channel, a coastal-type wave absorber was employed, and the slope of the wave maker was set to 20%. The coastal-type wave absorber within the wave channel is shown in Figure 4.



Figure 4. Coastal type wave absorber

To visualize and control the waves generated in the wave channel in real time, measurements were taken at two different points along the channel. An electronic measurement system equipped with Wallingford resistivity probe sensors was utilized. The first probe was positioned 14 meters from the resting position of the wave maker, and the second probe was located 17 meters away from the wave maker. The probe setup used for wave measurement is shown in Figure 5. Measurements were conducted with a sampling frequency of 50 Hz, within a ± 10 V range, and with 15-bit resolution. A LabVIEW interface was developed for the numerical analysis and visualization of the results. All recorded signals were analyzed in the frequency domain using the Fast Fourier Transform (FFT).

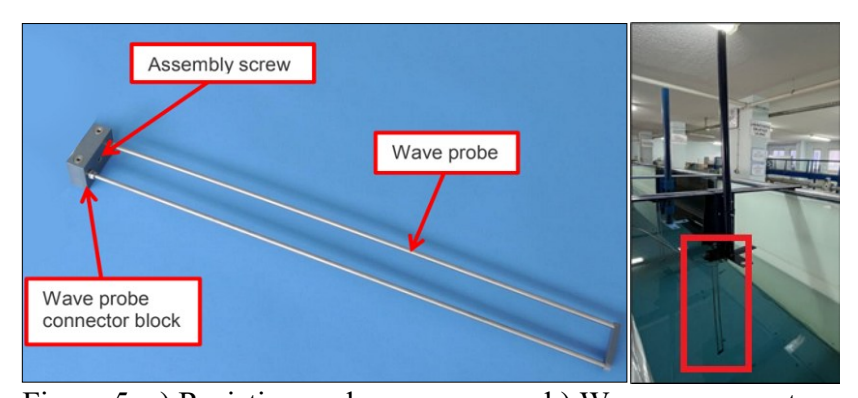


Figure 5. a) Resistive probe wave gauge b) Wave gauge system

2.2. Energy transformation

The wave generation principle of the piston-type wave maker within the wave channel is schematically illustrated in Figure 6. In this figure, key parameters such as the piston stroke "S(t)", wave height "H", wavelength "lambda (λ)", and water depth "h" are defined. The wave propagates in the "x" direction, while the vertical axis is taken as "z", and vertical displacements along the free surface of the wave are analyzed.

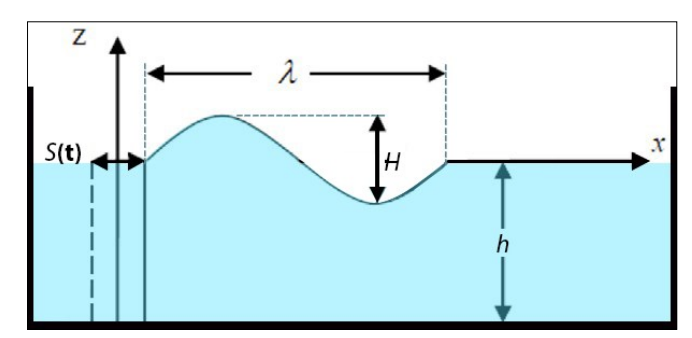


Figure 6. Piston-type wave maker

Piston Stroke "S(t)": The wave maker consists of a piston that moves back and forth through a hydraulic servo cylinder. The position of the piston at time "t" is expressed as the stroke value "S(t)". As the piston reaches its maximum stroke, it pushes and pulls the water mass, enabling wave formation.

Water Depth "h": The water depth in the wave channel refers to the distance from the bottom to the free surface. In this study, the "h" value was fixed at 50 cm and 60 cm for the regular wave experiments.

For the wave generation structure shown in Figure 1, the characteristic properties of the wave are defined as "wave height," "wavelength," and "wave period."

Wave Height "H": The vertical distance between the wave crest and the wave trough. If the wave amplitude is "a," then H=2a.

Wavelength "lambda (λ)": The horizontal distance between two consecutive wave crests or troughs, representing the spatial period of the wave.

Wave Period "T": The time required for one complete wave cycle to occur. The frequency is defined as f=1/T, and the angular frequency is given by $\omega=2\pi f$.

The piston-type wave maker in the wave channel has a total stroke range of 400 mm. In this study, water waves generated at different piston stroke values will be analyzed using control signals with varying amplitudes and frequencies.

2.3. Wave channel controller hardware

A proportional directional control valve was used to control the hydraulic cylinder in the wave channel for forward or backward motion at the desired stroke values. The directional control valve was actuated by the controller via the NI-9263 module, operating within a ±10V range. The position of the hydraulic cylinder was transmitted to the controller through an LVDT providing a 4–20 mA output, connected to the NI-9215 module. The NI-9074 packaged controller (PAC) was utilized as the control system. The NI-9074 includes an integrated Xilinx Spartan-3 FPGA, which was selected as the hardware controller for the wave generation system. FPGA are parallel and customizable platforms designed to execute advanced processing and control tasks at hardware-level speeds. Fundamentally, an FPGA is a programmable chip comprising three primary components: logic blocks, programmable interconnects, and I/O blocks.

The synthesis of FPGA Virtual Instrument (VI) structures with physical hardware in LabVIEW differs from traditional LabVIEW for Windows or LabVIEW Real-Time applications. While the structure of the LabVIEW code remains similar to that of other targets, clicking the "Run" button in the LabVIEW software initiates a distinct process for FPGA targets. First, LabVIEW FPGA generates VHDL code, which is passed to the Xilinx compiler. The Xilinx compiler then synthesizes the VHDL code, incorporates all synthesized components into a bitstream file, and routes them accordingly. Finally, the "bitstream file" created by LabVIEW is loaded onto the FPGA, enabling it to achieve its programmed functionality [12]. The technical specifications of the NI-9074 PAC are presented in Table 1.

Table 1. NI-CRIO9074 FPGA technical specifications[20]

| Feature | Specification |
|------------------------|---------------------------------------|
| Processor | 400 MHz Freescale MPC5200 real-time |
| | processor |
| FPGA | Xilinx Spartan-3 2M gates FPGA |
| Memory (RAM) | 128 MB DRAM |
| Storage (Flash Memory) | 256 MB |
| I/O Module Slots | 8 hot-swappable C Series module slots |
| Ethernet Port | 2 |
| Operating System | NI Real-Time OS |
| Programming Languages | LabVIEW, C/C++, NI Scan Engine |

To control the stroke of the hydraulic cylinder within the desired range, a sinusoidal input signal was generated in the LabVIEW FPGA environment. By entering parameters such as amplitude, frequency, and offset, the hydraulic cylinder was able to track the input signal using proportional control techniques. The NI-9215 analog input module and the NI-9263 analog output module, both compatible with the NI-9074 PAC, were employed. The NI-9263 module provided output signals within a ±10V range. The voltage signal generated in the software was used to electronically control the proportional directional control valve within the hydraulic cylinder control system, enabling the hydraulic cylinder's operation. The hydraulic cylinder has a motion range of 0–700 mm, and analog voltage signals from the LVDT integrated into the cylinder were transmitted to the FPGA via the NI-9215 module. This same module was also utilized for wave measurement. The control diagram of the FPGA-based wave channel system is shown in Figure 7. By performing position control of the hydraulic cylinder, the piston-type wave maker was actuated, producing regular water waves within the wave channel.

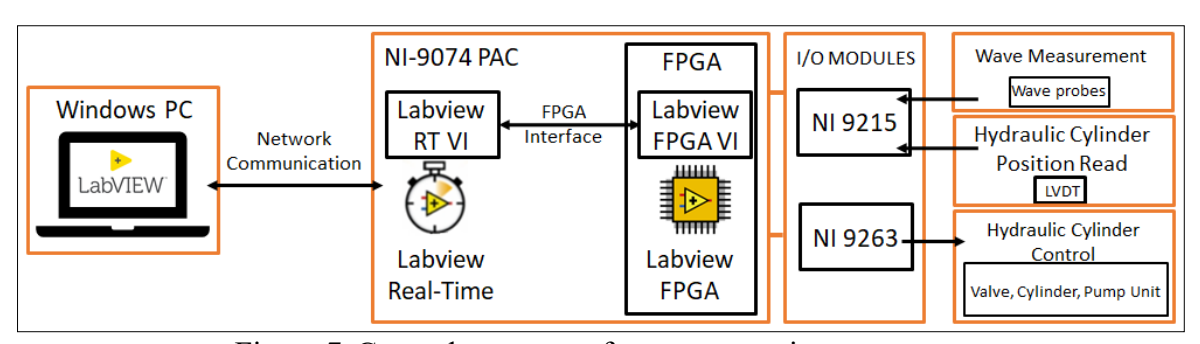


Figure 7. General structure of wave generating system

2.4. Model of the hydraulic system

To achieve position control of the hydraulic system in the wave channel, system identification was performed using the black-box method. The stimulus signal provided in Equation 1 was applied to the hydraulic directional control valve via the NI-CRIO 9074 PAC, and the position data of the hydraulic cylinder were recorded. Signals were collected for the model identification process, and no software-based controller was utilized in this configuration. The programming was solely designed to capture the position signal corresponding to the applied voltage signal.

$$y = 1.1(\sin 2\pi (0.05 * t)) + 0.5(\sin 2\pi (0.2 * t)) + 0.8(\sin 2\pi (t))$$
 (1)

The hydraulic cylinder used in the wave channel structure was selected as a double-acting, double-rod servo cylinder. This configuration minimizes speed variations during the forward and backward movements of the hydraulic cylinder. The proportional directional control valve in the hydraulic system was supplied with hydraulic fluid at a constant pressure of 50 bar by a fixed-displacement hydraulic unit with a power capacity of 4 kW. The generalized control diagram of the hydraulic system is shown in Figure 8.

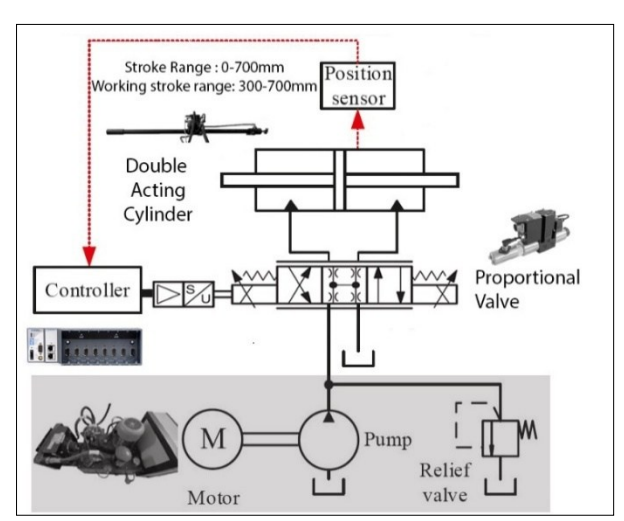


Figure 8. Hydraulic system

The control software developed for the identification of the hydraulic system operated at a cycle rate of one millisecond. The hydraulic cylinder could move within a range of 0–700 mm; however, due to the piston-type wave maker structure in the wave channel, the working range was set to 300–700 mm. The resting position of the hydraulic cylinder was defined as 500 mm, and the starting position for the system identification process was set at 250 mm. The data obtained were transferred to the Matlab/System Identification Toolbox (SIT) software, where the system model was created. Simulation studies showed that the highest model accuracy was achieved with a third-order state-space model, with 95.2% model prediction accuracy and 95.54% model fit.

Here, \dot{x} (t) represents the system's state vector, u(t) denotes the input signal, and y(t) corresponds to the output variable. The model, provided in Equation 2 and Equation 3, was defined using experimental data and derived to be valid within a linear operating range.

$$\dot{\mathbf{x}}(t) = A \cdot \mathbf{x}(t) + B \cdot \mathbf{u}(t) \tag{2}$$

$$y(t) = C \cdot x(t) + D \cdot u(t) \tag{3}$$

In the third-order state-space model obtained using the Matlab/SIT, the "A" matrix represents the interactions between the hydraulic cylinder and its associated components, such as cylinder chamber pressure, piston position, and piston velocity. The "B" matrix describes how the input signal applied to the hydraulic proportional directional control valve influences the state variables. The matrices "A" and "B" for the model are provided in Equation 4.

$$A = \begin{bmatrix} 0.002 & 0.0983 & -0.2235 \\ -0.1674 & -83.3994 & 1.1828x10^{3} \\ -0.0492 & 22.7009 & -1.0873x10^{3} \end{bmatrix}, B = \begin{bmatrix} -2.3107x10^{-4} \\ 1.2604 \\ -1.4932 \end{bmatrix}$$
(4)

In the state-space model, the "C" matrix determines which state variables are measured and evaluated as the system output (e.g., piston position). The "D" matrix defines the effect that the input signal can have directly on the output, bypassing the state variables. In many hydraulic systems, the "D" value is typically zero or very small because the immediate effect of the input is primarily reflected through the state variables. The "C" and "D" matrices for the model are provided in Equation 5.

$$C = [-9.6468x10^4 \ 2.3579 - 6.5201], D = 0$$
 (5)

The elements of the K matrix are determined by MATLAB/SIT to account for the disturbance effects acting on the hydraulic system during the modeling process. The values of the K matrix are provided in Equation 6. Its incorporation into the obtained system model is presented in Equation 7 and Equation 8.

$$K = \begin{bmatrix} -0.0061 \\ -8.4178 \\ 1.7921 \end{bmatrix} \tag{6}$$

$$\dot{\mathbf{x}}(t) = A \cdot \mathbf{x}(t) + B \cdot \mathbf{u}(t) + K.\,\mathbf{e}(t) \tag{7}$$

$$y(t) = C \cdot x(t) + D \cdot u(t) + e(t)$$
(8)

A PI controller has been chosen for the precise control of the hydraulic system. The PI controller adapts to the dynamic characteristics of the hydraulic system, providing high accuracy in position control. The proportional gain " K_p " and integral gain " K_i " coefficients are used to optimize the system's stability and response speed. The " K_p " coefficient accelerates the system's response, minimizing the error between the reference signal and the actual system output. Increasing the proportional gain allows the system to respond more quickly, but excessively high " K_p " values may lead to instability. The " K_i " coefficient, on the other hand, eliminates the steady-state error component in the system response, enabling the system to reach the desired steady-state condition. The integral gain improves the long-term alignment of the system with the reference signal; however, excessively high " K_i " values may cause oscillations or slow stabilization in the system.

For the control of the hydraulic system, the PI controller parameters were determined using the third-order state-space model of the hydraulic system created in Simulink.

Initially, the PI controller parameters were set to K_p =0 and K_i =0, and the system's response was observed. Subsequently, the K_p and K_i parameters were gradually increased to optimize the closed-loop system's behavior. During the simulation process, the accuracy and stability of the hydraulic cylinder's position control were analyzed. The values of K_p =0.255 and K_i =0.15 obtained from the simulation environment were integrated into the real system. It was verified that the PI controller adapted to the dynamic characteristics of the hydraulic system and exhibited the desired performance.

2.5. FPGA based control software

In this study, the position control of the piston-type wave maker mechanical system, used to generate waves consisting of a single frequency and amplitude component, is achieved through a hydraulic cylinder system. A proportional directional control valve is employed for the position control of the hydraulic cylinder. The user provides the amplitude and frequency parameters of the hydraulic cylinder directly through a LabVIEW program developed for this purpose. The front panel interface of the wave channel control software developed in LabVIEW is shown in Figure 9. In the initial program, the Virtual Instrument (VI) operating on the computer directly transfers the hydraulic cylinder parameters to the FPGA target. If desired, the user can also control the LabVIEW program running on the FPGA target.

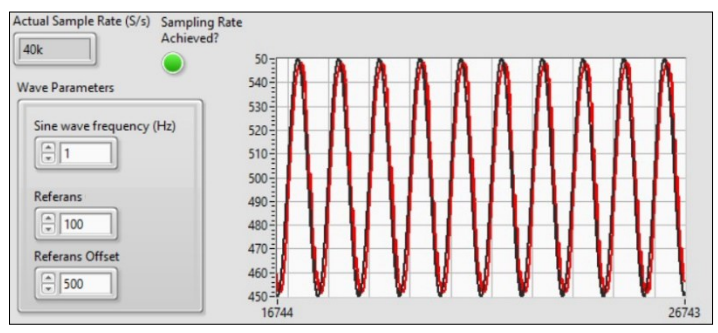


Figure 9. Labview interface developed for transferring the control parameters of the cylinder to the FPGA structure

The program panel (back panel) corresponding to the interface (front panel) shown in Figure 9 is presented in Figure 10.

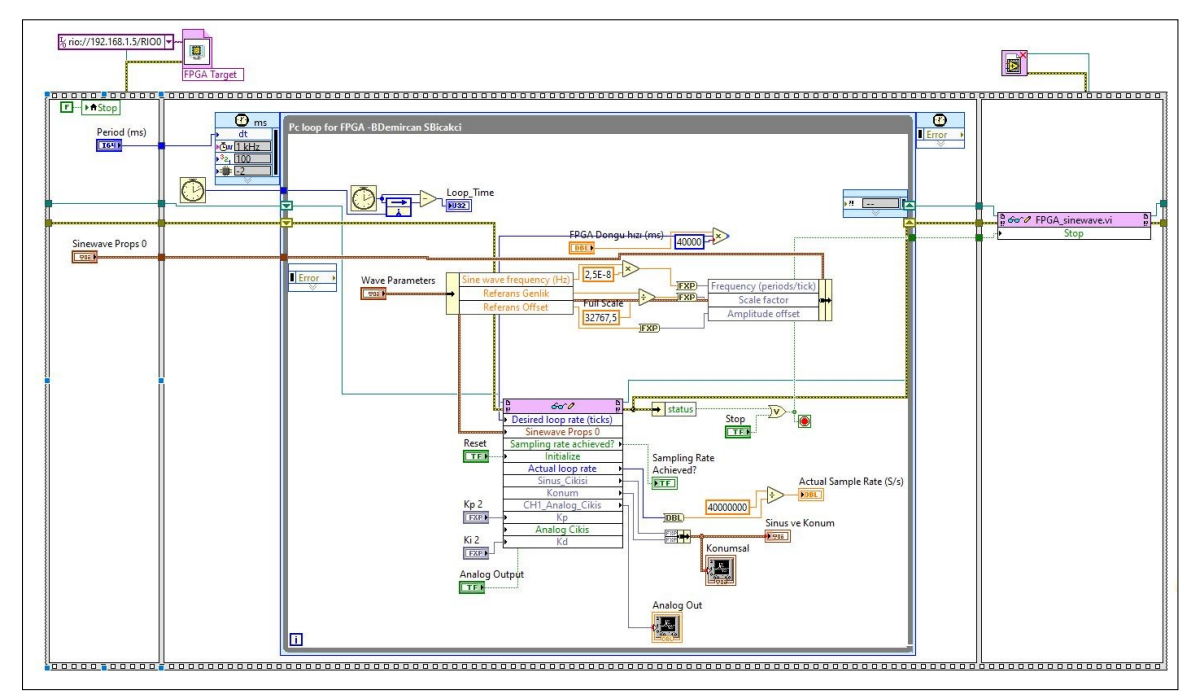


Figure 10. Labview interface developed for transferring the control parameters of the cylinder to the FPGA structure-back panel

The FPGA parameters provided by the user are directly transferred to the FPGA structure and can also be monitored by the user through the FPGA interface. The loop rate for wave generation in the developed LabVIEW software was set to 25 microseconds. Apart from the FPGA structure, the "scan engine" operating within the NI-CRIO 9074 hardware can run at a maximum loop rate of 1 millisecond. The LabVIEW software running directly on the FPGA is shown in Figure 11.

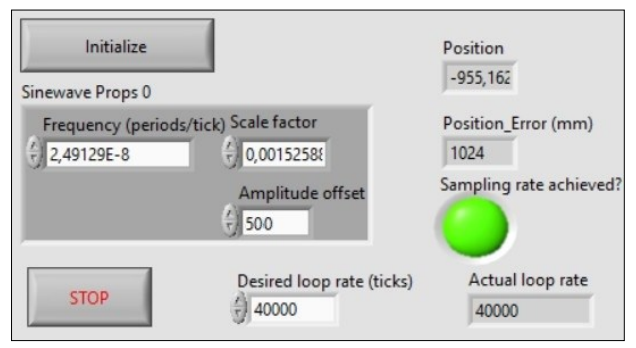


Figure 11. FPGA-based Labview program developed for the control of the piston type wave maker

Similar to the LabVIEW structure on the computer side, the LabVIEW program running on the FPGA also includes a back panel and a front panel. The back panel corresponding to the front panel shown in Figure 11 is presented in Figure 12.

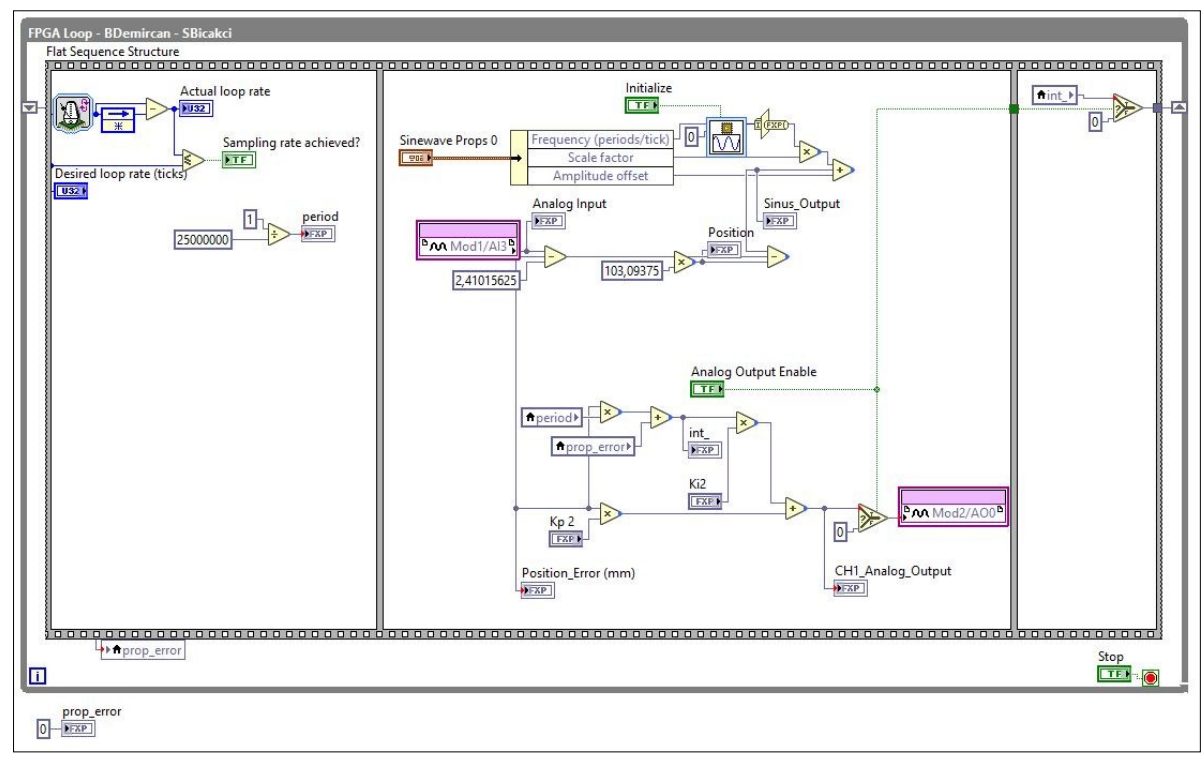


Figure 12. FPGA-based Labview program developed for the control of the piston type wave maker-back panel

2.6. Wave measurement

Since the wave maker in the wave channel operates with a single amplitude and frequency component, the generated waves are in a regular form. In this case, no spectrum transformation was necessary, as the wave frequency matched the control signal frequency of the hydraulic cylinder. Therefore, it was sufficient to measure wave heights directly from the data obtained via wave measurement probes. Figure 13 shows the graph obtained from the first wave measurement probe sensor for waves generated by the wave maker under a 1 Hz control signal.

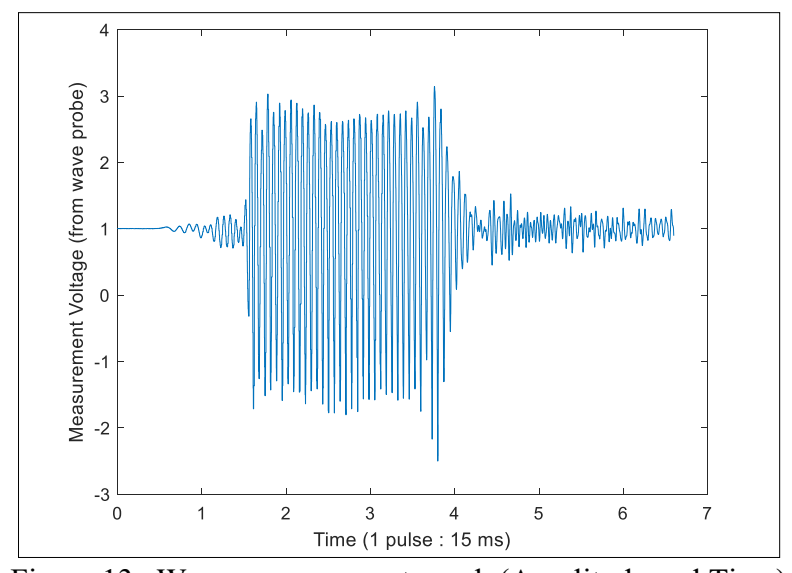


Figure 13. Wave measurement graph (Amplitude and Time)

Real-time wave measurements obtained from the first wave measurement probe sensor were analyzed using the Fast Fourier Transform (FFT) to determine the frequency information of the generated wave. The frequency spectrum of the signal after applying the FFT is shown in Figure 14.

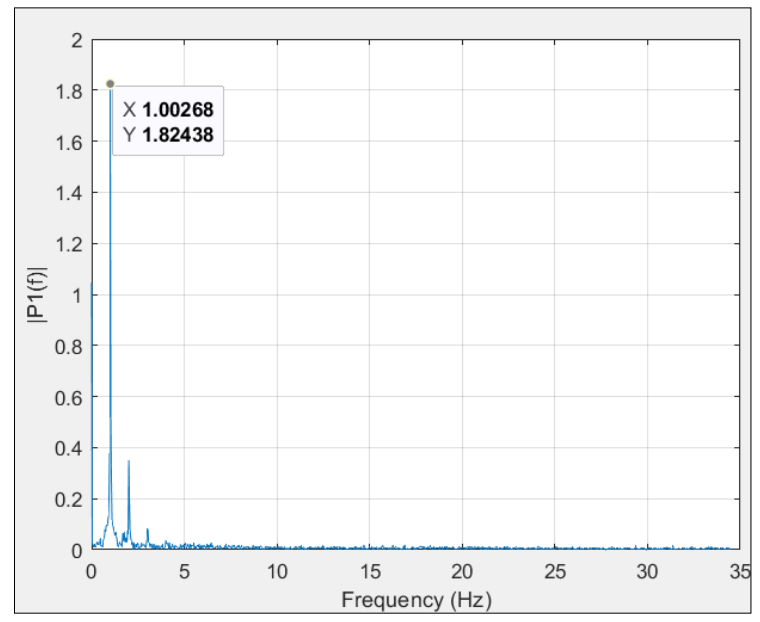


Figure 14. FFT graph of wave measurements

According to the FFT analysis results, the frequency of the wave profile generated under a 1 Hz control signal was measured as 1 Hz, matching the frequency of the control signal.

3. Results

The hydraulic cylinder system and the piston-type wave maker in the wave channel were controlled using the PI control method. According to the experiment presented in Table 2, the measurement results obtained from the sensor used for wave measurement, along with the hydraulic cylinder stroke values and constant water depth data, were recorded for a control signal frequency of 0.8 Hz.

| Table 2. Wave Channel Experiment Results-1 | | | | | | |
|--|--|--------------------------------|------------------------------------|--|--|--|
| Constant Water Level [h]-cm | Hydraulic Cylinder Total Stroke [S(t)]- cm | Wave Height [<i>H</i>]-cm | Hydraulic Cylinder Frequency-Hz | | | |
| 50 | 1.6 | 2.5 | 1 | | | |
| 50 | 3.6 | 5 | 1 | | | |
| 50 | 5.4 | 8 | 1 | | | |
| 50 | 7.6 | 10 | 1 | | | |
| 50 | 9.6 | 13 | 1 | | | |
| 50 | 11.6 | 16 | 1 | | | |
| 60 | 1.6 | 2.9 | 1 | | | |
| 60 | 3.6 | 5 | 1 | | | |

Table 2. Wave Channel Experiment Results-I

Table 2. Wave Channel Experiment Results-I

| Constant Water Level [h]-cm | Hydraulic Cylinder Total Stroke [S(t)]- cm | Wave Height [<i>H</i>]-cm | Hydraulic Cylinder Frequency-Hz |
|--------------------------------|--|-----------------------------|------------------------------------|
| 60 | 5.4 | 8 | 1 |
| 60 | 7.6 | 11 | 1 |
| 60 | 9.6 | 15 | 1 |
| 60 | 11.6 | 17 | 1 |

Table 3. Wave Channel Experiment Results-II

| Constant Water Level [h]-cm | Hydraulic Cylinder Total Stroke [S(t)]- cm | Wave Height [<i>H</i>]-cm | Hydraulic Cylinder Frequency-Hz |
|--------------------------------|--|--------------------------------|------------------------------------|
| 50 | 1.6 | 1 | 0.8 |
| 50 | 3.6 | 3 | 0.8 |
| 50 | 5.4 | 5 | 0.8 |
| 50 | 7.6 | 7 | 0.8 |
| 50 | 9.6 | 8 | 0.8 |
| 50 | 11.6 | 11 | 0.8 |
| 60 | 1.6 | 1.6 | 0.8 |
| 60 | 3.6 | 4 | 0.8 |
| 60 | 5.4 | 5.7 | 0.8 |
| 60 | 7.6 | 8 | 0.8 |
| 60 | 9.6 | 11 | 0.8 |
| 60 | 11.6 | 12 | 0.8 |

The hydraulic cylinder system and piston-type wave maker in the wave channel were controlled using the PI control method. According to the experiment presented in Table 2, the measurement results obtained from the sensor used for wave measurement were provided for a control signal frequency of 0.8 Hz, along with the hydraulic cylinder stroke values and constant water depth data.

Tables 2 and 3 summarize the effects of the total stroke of the hydraulic cylinder (ranging from 1.6 cm to 11.6 cm) and cylinder frequency (1 Hz or 0.8 Hz) on the resulting wave height under constant water depths (50 cm or 60 cm) in the wave channel. Based on the results:

Effect of Stroke Increase: As the hydraulic cylinder stroke increases, the generated wave height systematically rises. For instance, at a water depth of 50 cm and a frequency of 1 Hz, a stroke of 1.6 cm produces a wave height of approximately 2.5 cm, whereas increasing the stroke to 11.6 mm raises the wave height to 16 cm. Similarly, at a depth of 60 cm and a frequency of 1 Hz, the wave height increases from 2.9 cm at 1.6 cm stroke to 17 cm at 11.6 cm stroke.

Effect of Water Depth: Comparing water depths of 50 cm and 60 cm reveals that, for the same stroke and frequency values, wave heights are generally slightly higher at 60 cm depth. For example, at 1 Hz frequency and 5.6 cm stroke, a wave height of 8 cm is achieved at 50 cm depth, while a height of 8.1 cm or higher is observed at 60 cm depth.

Effect of Frequency (0.8 Hz vs. 1 Hz): As shown in Table 3, reducing the frequency to 0.8 Hz results in wave heights that are comparatively lower than those generated at 1 Hz for similar stroke values. For example, at a depth of 50 cm and a stroke of 5.6 cm, a wave height of 8 cm is achieved at 1 Hz, whereas a height of approximately 5 cm is observed at 0.8 Hz.

Evaluation and Applications: The experimental results demonstrate that cylinder stroke and frequency are key determinants of wave formation. Higher stroke values and frequencies increase wave height, allowing for a broader range of desired wave parameters to be achieved. Although increasing water depth has a moderately positive effect on wave height, optimizing parameters such as channel length, water level, stroke range, and frequency collectively is necessary for efficient system operation. These findings provide a critical foundation for controlled wave generation in wave channels. In particular, evaluating these parameters together facilitates more accurate predictions of wave behavior, which is essential for testing wave energy converters under varying conditions or designing coastal and offshore structures.

4. Conclusion and discussion

In this study, a hydraulically controlled piston-type wave generator was successfully implemented in a 24 m \times 1 m wave channel using the NI-CRIO 9074 PAC equipped with FPGA hardware. The experimental results demonstrated that adjusting the hydraulic cylinder stroke and actuation frequency allowed for the generation of regular waves over a wide range of amplitudes. Specifically, increasing the cylinder stroke systematically elevated the wave height, while variations in water depth (50 cm and 60 cm) and frequency (1 Hz and 0.8 Hz) significantly influenced wave formation. These findings confirm that optimizing key parameters such as stroke, frequency, and water depth is essential for achieving the desired wave characteristics and minimizing wave reflections within the channel.

Additionally, the FPGA-based control approach enabled real-time and precise management of the hydraulic cylinder, ensuring stable wave production with minimal latency. Experimental data obtained via resistive wave probes placed at different locations along the channel verified that the generated waves closely matched the predicted input signals in terms of amplitude and frequency. This platform, therefore, provides a robust and flexible environment for evaluating wave-structure interactions in areas such as wave energy converters, coastal defense systems, and offshore platforms.

Overall, this study highlights the importance of advanced real-time control strategies, such as FPGA-based architectures, in improving wave channel experiments. Future research could focus on employing more sophisticated or adaptive control algorithms, such as model predictive or machine learning-based controllers, to enhance wave quality and expand the range of operational conditions. By integrating these advancements, wave

channels can become even more powerful experimental platforms for both fundamental scientific research and the development of practical marine renewable energy technologies.

References

- [1] M. A. Zullah, D. Prasad, M. R. Ahmed, and Y. H. Lee, Performance analysis of a wave energy converter using numerical simulation technique, *Science China Technological Sciences*, vol. 53, no. 1, pp. 13–18, Jan. 2010. doi: 10.1007/S11431-010-0026-3.
- [2] Q. Du and D. Y. C. Leung, 2D Numerical Simulation of Ocean Waves, *Proceedings of the World Renewable Energy Congress*, 8–13 May 2011, Linköping, Sweden, vol. 57, pp. 2183–2189, Nov. 2011. doi: 10.3384/ECP110572183.
- [3] H. Gao and B. Li, Establishment of Motion Model for Wave Capture Buoy and Research on Hydrodynamic Performance of Floating-Type Wave Energy Converter, *Polish Maritime Research*, vol. 22, no. s1, pp. 106–111, Sep. 2015. doi: 10.1515/POMR-2015-0041.
- [4] G. Rajapakse, S. Jayasinghe, and A. Fleming, Power Smoothing and Energy Storage Sizing of Vented Oscillating Water Column Wave Energy Converter Arrays, *Energies*, vol. 13, no. 5, p. 1278, Mar. 2020. doi: 10.3390/EN13051278.
- [5] G. Giannini, P. Rosa-Santos, V. Ramos, and F. Taveira-Pinto, On the Development of an Offshore Version of the CECO Wave Energy Converter, *Energies*, vol. 13, no. 5, p. 1036, Feb. 2020. doi: 10.3390/EN13051036.
- [6] M. A. Jusoh, M. Z. Ibrahim, M. Z. Daud, A. Albani, and Z. M. Yusop, Hydraulic Power Take-Off Concepts for Wave Energy Conversion System: A Review, *Energies*, vol. 12, no. 23, p. 4510, Nov. 2019. doi: 10.3390/EN12234510.
- [7] A. Maria-Arenas, A. J. Garrido, E. Rusu, and I. Garrido, Control Strategies Applied to Wave Energy Converters: State of the Art, *Energies*, vol. 12, no. 16, p. 3115, Aug. 2019. doi: 10.3390/EN12163115.
- [8] H. Carreno-Luengo and A. Camps, Empirical Results of a Surface-Level GNSS-R Experiment in a Wave Channel, *Remote Sensing*, vol. 7, no. 6, pp. 7471–7493, Jun. 2015. doi: 10.3390/RS70607471.
- [9] I. Gyongy, J.-B. Richon, T. Vruce, and I. Bryden, Synteza i aktywność biologiczna nowych analogów tiosemikarbazonowych chelatorów żelaza, *Physical Processes*, Technomics Press, pp. 343–354, 2013. doi: 10.2/JQUERY.MIN.JS.
- [10] T. Kawaguchi, K. Nakano, S. Miyajima, and T. Arikawa, A Theory for Wave Energy Conversion by Bottom-Mounted Oscillating Bodies, (2024). https://www.researchgate.net/publication/334031823 A Theory for Wave Energy Conversion by Bottom-Mounted Oscillating Bodies, (07.01.2025).
- [11] B. Chenari, S. S. Saadatian, and A. D. Ferreira, Numerical Modelling of Regular Waves Propagation and Breaking Using Waves2Foam, *Journal of Clean Energy Technologies*, vol. 3, no. 4, pp. 276–281, 2015. doi: 10.7763/JOCET.2015.V3.208.
- [12] M. Renganathan and M. Hossain, Numerical Analysis of a Horizontal Pressure Differential Wave Energy Converter, *Energies*, vol. 15, no. 20, p. 7513, Oct. 2022. doi: 10.3390/EN15207513.

- [13] X. Tian, Q. Wang, G. Liu, W. Deng, and Z. Gao, Numerical and experimental studies on a three-dimensional numerical wave tank, *IEEE Access*, vol. 6, pp. 6585–6593, Jan. 2018. doi: 10.1109/access.2018.2794064.
- [14] M. Y. Khalid, Laboratory Experiments on Water Wave Generation, PhD Thesis, University of Dundee, United Kingdom, (2020).
- [15] M. Beneduce, Design of a Wavemaker for the Water Tank at the Politecnico di Torino, Maser Thesis, Politecnico Di Torino, Italy, (2018).
- [16] L. F. Su, A. F. Zhang, and X. Liang, Research of the Servo Motion Control of Wave Maker, *Applied Mechanics and Materials*, vol. 541–542, pp. 1243–1247, 2014. doi: 10.4028/www.scientific.net/amm.541-542.1243. (07.01.2025).
- [17] Y. Jian-jun, D. Duo-tao, J. Gui-lin, and L. Sheng, High Precision Position Control of Electro-Hydraulic Servo System Based on Feed-Forward Compensation, (2024).

 https://www.researchgate.net/publication/289452217_High_Precision_Position_Control_of_Electro-Hydraulic_Servo_System_Based_on_Feed-Forward Compensation, (07.01.2025).
- [18] T. G. Ling, M. F. Rahmat, and A. R. Husain, System identification and control of an Electro-Hydraulic Actuator system, *Proceedings 2012 IEEE 8th International Colloquium on Signal Processing and Its Applications*, pp. 85–88, 2012. doi: 10.1109/CSPA.2012.6194696.
- [19] M. S. Mahdi, Controlling a Nonlinear Servo Hydraulic System Using PID Controller with a Genetic Algorithm Tool, (2024). https://www.researchgate.net/publication/311536154 Controlling a Nonlinear Servo Hydraulic System Using PID Controller with a Genetic Algorithm Tool, (07.01.2025).
- [20] Emerson, LabVIEW for CompactRIO Developer's Guide NI., (2024). https://www.ni.com, (07.01.2025).